

ENERGY TRANSFER PHENOMENA IN $\text{GdMgB}_5\text{O}_{10}$

Markku Leskelä *, Michel Saakes and George Blasse,
Physical Laboratory,
State University, P.O. Box 80.000, 3508 TA Utrecht, The Netherlands

(Received September 22, 1983; Communicated by W. B. White)

ABSTRACT

The luminescence of Mn^{2+} , Bi^{3+} , Ce^{3+} and Tb^{3+} in $\text{GdMgB}_5\text{O}_{10}$ and some codoped materials is reported. Energy transfer rates are derived from the experiments. The $\text{Bi}^{3+} \rightarrow \text{Gd}^{3+}$ and $\text{Gd}^{3+} \rightarrow \text{Bi}^{3+}$ transfer rates are about equal at room temperature. The excitation energy is able to migrate among the Gd^{3+} sublattice. The Ce^{3+} ion is a good sensitizer for this sublattice. By diluting the Gd^{3+} sublattice with La^{3+} ions, the energy migration in Gd^{3+} zig-zag chains was blocked and interchain energy transfer occurred. Very efficient phosphors can be obtained by using Ce^{3+} as a sensitizer, the Gd^{3+} sublattice as an intermediary and Tb^{3+} as an activator.

Introduction

The crystal structure of $\text{LaMgB}_5\text{O}_{10}$ has been described recently (1). It contains linear zig-zag chains of La^{3+} ions. The shortest $\text{La}^{3+} - \text{La}^{3+}$ intrachain-distance is about 4 Å, the shortest interchain-distance about 6.4 Å. The same structure is observed for these borates with smaller lanthanide ion down to Er^{3+} .

Recently we have described the Bi^{3+} and Mn^{2+} emission in $\text{LaMgB}_5\text{O}_{10}$, together with some energy transfer phenomena (2). In this paper we report our results for $\text{GdMgB}_5\text{O}_{10}$. Similar activator ions were investigated, viz. Mn^{2+} , Bi^{3+} , and in addition Ce^{3+} and Tb^{3+} . One of our aims was to detect energy migration in the Gd^{3+} sublattice which may be one-dimensional. Such one-dimensional energy migration has been observed for $\text{EuMgB}_5\text{O}_{10}$ and $\text{TbMgB}_5\text{O}_{10}$ (3). It turned out that several interesting energy transfer phenomena appear

* On leave from Depts. of Chemistry, University of Oulu and Helsinki University of Technology, Finland.

in $\text{GdMgB}_5\text{O}_{10}$. The one-dimensional character was lost upon diluting the Gd^{3+} sublattice with La^{3+} . After completing this work we became aware of work by De Hair and Van Kemenade on the role of similar materials in fluorescent lamps (4).

Experimental

The experimental techniques were the same as described before (2).

Results and discussion

$\text{GdMgB}_5\text{O}_{10}$: Mn

The Mn^{2+} ion in $\text{GdMgB}_5\text{O}_{10}$ replaces Mg^{2+} which has a distorted octahedral coordination. It gives a red emission, the spectral energy distribution of which is equal to that of Mn^{2+} in $\text{LaMgB}_5\text{O}_{10}$ (2). The excitation spectrum, however, is different because we observe, in addition to the characteristic Mn^{2+} bands (2), strong excitation bands which are due to Gd^{3+} , viz. the transitions $^8\text{S} \rightarrow ^6\text{P}$, ^6I and ^6D . This shows that excitation into the Gd^{3+} ion results in Mn^{2+} emission, i.e. $\text{Gd}^{3+} \rightarrow \text{Mn}^{2+}$ energy transfer occurs.

At room temperature (RT) the total emission for Gd^{3+} excitation consists of 96% Mn^{2+} and 4% Gd^{3+} emission for a sample with 1% Mn. The Gd^{3+} emission ($^6\text{P} \rightarrow ^8\text{S}$ at about 315 nm) overlaps the Mn^{2+} absorption bands (2) in an unfavourable way. In connection with the low oscillator strengths of the optical transitions involved, this restricts the $\text{Gd}^{3+} \rightarrow \text{Mn}^{2+}$ transfer to very short distances, probably nearest neighbours only (3.6 Å, ref. 1). If the transfer occurs by exchange, it will be restricted to short distances also. The high amount of Mn^{2+} emission at RT, together with the short distance range of the $\text{Gd}^{3+} \rightarrow \text{Mn}^{2+}$ transfer, shows that energy migration among the Gd^{3+} sublattice occurs.

Unfortunately we were not able with the present set-up to measure the decay times of the Gd^{3+} emission. It seems not unreasonable to assume that the radiative decay time of Gd^{3+} in $\text{GdMgB}_5\text{O}_{10}$ is about equal to that of Gd^{3+} in $\text{YAl}_3\text{B}_4\text{O}_{12}$ (5), viz. about 10^{-3} s. We can also take the $\text{Gd}^{3+} \rightarrow \text{Gd}^{3+}$ transfer probability from that work, viz. $\sim 10^7$ s $^{-1}$. Because the $\text{Gd}^{3+} \rightarrow \text{Mn}^{2+}$ nearest-neighbour transfer rate cannot be much larger than the Gd^{3+} radiative rate, we estimate it to be 10^4 s $^{-1}$ or less. The comparison of these transfer rates learns that at RT we are dealing with the case of fast diffusion, i.e. the transfer from Gd^{3+} to Mn^{2+} is much slower than to Gd^{3+} . Although we have no experimental proof for this, it is clear that this diffusion should be strongly one-dimensional, i.e. in the chains. Note that the Mn^{2+} ions are not in the chain. The amount of Mn^{2+} emission in the total luminescence output can be used to find the total transfer rate to the Mn^{2+} ions. The ratio of the amounts of Mn^{2+} and Gd^{3+} emission (~ 25) is equal to the ratio of this total transfer rate to the Gd^{3+} radiative rate ($\sim 10^3$ s $^{-1}$). Therefore the total

transfer rate is about $2 \cdot 10^4 \text{ s}^{-1}$. From this value and the Mn^{2+} concentration it follows that the $\text{Gd}^{3+} \rightarrow \text{Mn}^{2+}$ transfer rate for nearest neighbours is $2 \cdot 10^6 \text{ s}^{-1}$. This means that the fast diffusion model is still approximately correct, but that the $\text{Gd}^{3+} \rightarrow \text{Mn}^{2+}$ transfer rate is considerably larger than estimated before. It seems very probable that this implies that this transfer occurs by exchange.

At low temperatures the amount of Mn^{2+} emission decreases: at 300 K it was 96%, at 40 K 66%, at 20 K 57%, at 9 K 50%. In addition we observed at 9 K a small amount of Tb^{3+} emission (< 1%). In fig. 1 we had plotted the amount of

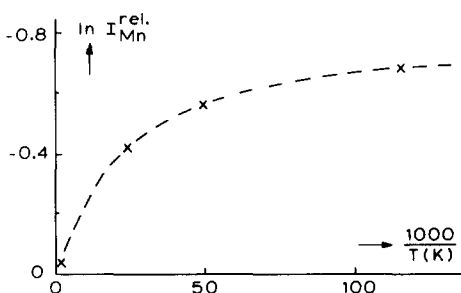


FIG. 1

The logarithm of the relative amount of Mn^{2+} emission ($I_{\text{Mn}}^{\text{rel}}$) of $\text{GdMg}_{0.99}\text{Mn}_{0.01}\text{B}_5\text{O}_{10}$ upon Gd^{3+} excitation plotted vs the reciprocal temperature (see also text).

Mn^{2+} emission logarithmically versus T^{-1} . No straight line is observed. This temperature dependence may be either due to a temperature dependence in the $\text{Gd}^{3+} \rightarrow \text{Gd}^{3+}$ transfer process or in the $\text{Gd}^{3+} \rightarrow \text{Mn}^{2+}$ transfer process. Due to the inhomogeneous broadening the Gd^{3+} migration is expected to be stopped at low temperatures. It is our experience (6) that such effects occur only below 20 K. The higher temperature effects observed here are therefore ascribed to a temperature dependence of the $\text{Gd}^{3+} \rightarrow \text{Mn}^{2+}$ transfer rate. In fact the Mn^{2+} excitation bands sharpen at lower temperatures which influences the spectral overlap. In the same way as described above the $\text{Gd}^{3+} \rightarrow \text{Mn}^{2+}$ transfer rate at these low temperatures is estimated to be 10^5 s^{-1} .

The small amount of Tb^{3+} emission in the low temperature spectra is due to the presence of a small amount of terbium in the starting material Gd_2O_3 . Its concentration may be about 10^{-5} m/o. If we take the 1% amount of Tb^{3+} emission, the $\text{Gd}^{3+} \rightarrow \text{Tb}^{3+}$ transfer rate is estimated in this way to be a few times 10^6 s^{-1} . We will return to $\text{Gd}^{3+} \rightarrow \text{Tb}^{3+}$ transfer below. We conclude that in $\text{GdMgB}_5\text{O}_{10} : \text{Mn}$ there is a rapid energy migration in Gd^{3+} chains if excitation is into the Gd^{3+} ions. When Mn^{2+} (or Tb^{3+}) are used as activators (traps), the emission spectrum is determined by the ratio of the Gd^{3+} radiative emission rate and the product of the individual trapping rate and the trap concentration (7).

GdMgB₅O₁₀ : Bi

Some peculiar observations were made for the case of Bi^{3+} -activated $\text{GdMgB}_5\text{O}_{10}$. Let us consider specifically the sample with composition $\text{Gd}_{0.97}\text{Bi}_{0.03}\text{MgB}_5\text{O}_{10}$. The Bi^{3+} spectra are known from our previous work on the lanthanum compound (2). First we consider our results observed at liquid helium temperature (LHeT).

At LHeT, excitation into the Bi^{3+} absorption band at 295 nm

($^1S_0 \rightarrow ^3P_1$) yields mainly Gd^{3+} emission at about 315 nm ($^6P \rightarrow ^8S$). Excitation into the Gd^{3+} levels (e.g. $^8S \rightarrow ^6I$ at 275 nm) yields only Gd^{3+} emission. From this we conclude that at LHeT we have efficient $Bi^{3+} \rightarrow Gd^{3+}$ transfer without any back transfer. This is confirmed by the fact that the excitation spectrum of the $^6P \rightarrow ^8S$ Gd^{3+} emission contains not only the Gd^{3+} absorption transitions, but also the Bi^{3+} absorption transition.

To discuss the $Bi^{3+} \rightarrow Gd^{3+}$ transfer we consider the relevant spectra (fig. 2). Note that the Bi^{3+} emission band at LHeT does not overlap the Gd^{3+} absorption line, which makes it hard, at first sight, to understand the appearance of energy transfer.

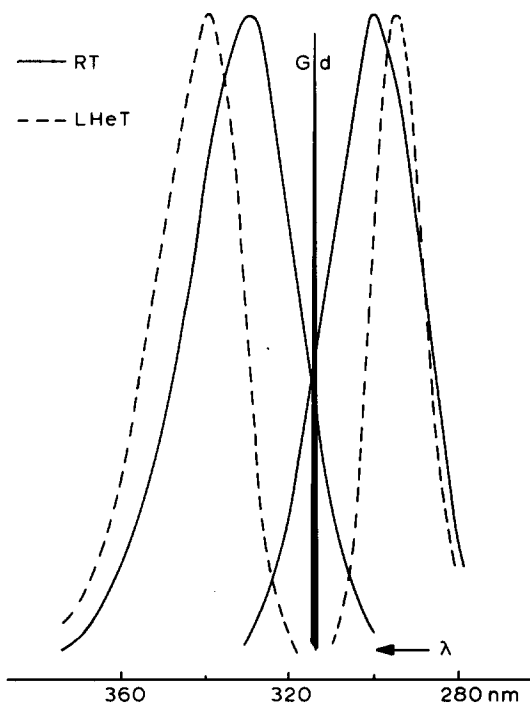


FIG. 2

Some spectral data of $Gd_{0.97}Bi_{0.03}MgB_5O_{10}$ at RT and LHeT. The line marked Gd indicates the Gd^{3+} emission and absorption line ($^8S - ^6P$). On the right hand side Bi^{3+} excitation spectra are given ($^1S_0 \rightarrow ^3P_1$) transition). On the left hand side Bi^{3+} emission spectra are given. The RT curve is real and corresponds to $^3P_1 \rightarrow ^1S_0$. The LHeT curve cannot be observed and is derived from the other curves. It corresponds to $^3P_0 \rightarrow ^1S_0$. See also text.

The way out of this is to assume that energy transfer occurs from the 3P_1 level of Bi^{3+} before it relaxes to the lower 3P_0 level. In fig. 2 we have drawn the RT emission band of the $^3P_1 - ^1S_0$ transition. This overlaps in fact the Gd^{3+} absorption. However, the nonradiative $^3P_1 \rightarrow ^3P_0$ rate was estimated to be $> 10^9 \text{ s}^{-1}$ (2), so that the transfer rate should be rather high. For electric dipole-dipole interaction we calculated the critical distance for transfer with a spectral overlap treatment (8). The result is $R_c = 5 \text{ \AA}$. For the shortest possible $Bi^{3+} - Gd^{3+}$ distance, viz. 4.0 \AA , this yields a transfer rate of $2 \times 10^7 \text{ s}^{-1}$, using the radiative $^3P_1 \rightarrow ^1S_0$ rate obtained earlier ($5 \times 10^6 \text{ s}^{-1}$, ref. 2). This transfer rate is obviously much too low to compete with the $^3P_1 \rightarrow ^3P_0$ nonradiative rate. This implies that the $Bi^{3+} \rightarrow Gd^{3+}$ transfer occurs by exchange. In view of the large extension of the excited $6s6p$ state of the Bi^{3+} ion and the short $Bi^{3+} - Gd^{3+}$ distance (4 \AA), transfer by exchange seems to be a good possibility.

At RT the situation is different. Excitation into the Bi^{3+} excitation band at 295 nm yields now mainly Bi^{3+} emission, whereas only about 2% of the total output is Gd^{3+} emission. However, also

excitation into the Gd³⁺ absorption band at 275 nm yields mainly Bi³⁺ emission and about 3% Gd³⁺ emission. Fig. 2 shows schematically the relevant emission and excitation spectra. Note the spectral overlap of ³P₁ → ¹S₀ Bi³⁺ emission and ⁸S → ⁶P Gd³⁺ absorption and that of ⁶P → ⁸S Gd³⁺ emission and ¹S₀ → ³P₁ Bi³⁺ absorption. Back transfer from Gd³⁺ → Bi³⁺ is clearly a possibility. It is illustrative to consider the extreme case in which the Bi³⁺ → Gd³⁺ transfer rate equals the Gd³⁺ → Bi³⁺ back transfer rate. Then the emission spectra should be independent of excitation wavelength if the transfer rates exceed the radiative rates. In view of our estimations above this is certainly the case. The ratio of Bi³⁺ and Gd³⁺ emission is determined by their radiative rates. At RT these are about 10⁶ s⁻¹ and 10³ s⁻¹, respectively (2,5). This gives a Gd³⁺/Bi³⁺ ratio of 3.10⁻² in view of the Bi³⁺ concentration (3%).

The RT situation is described rather well by this extreme situation. This means that the Gd³⁺ → Bi³⁺ transfer is strongly temperature dependent which is related to the temperature dependence of the spectral overlap involved (see fig. 2). On the other hand the Bi³⁺ → Gd³⁺ transfer is not strongly temperature dependent, since the spectral overlap does not vary as strongly as for the back-transfer case. At RT both rates are about equal.

Finally we note that the Bi³⁺ ion is not able to act as a sensitizer for the Gd³⁺ ions at RT. This is strikingly different for the Ce³⁺ ion as we will see now.

GdMgB₅O₁₀ : Ce

The luminescence of Ce³⁺ in LaMgB₅O₁₀ was reported by Saubat et al. (9). In GdMgB₅O₁₀, however, the Ce³⁺ ion was found to be nonluminescent. The reason for this is most easily found by codoping GdMgB₅O₁₀ with Ce³⁺ and Tb³⁺. For a sample with composition Gd_{0.977}Ce_{0.02}Tb_{0.003}MgB₅O₁₀ the excitation spectrum of the Tb³⁺ emission consists of very weak Tb³⁺ lines, weak Gd³⁺ lines and strong Ce³⁺ bands. This was observed at LHeT and RT. Direct transfer from Ce³⁺ to Tb³⁺ of any importance can be excluded in view of the results by Saubat et al. (9) and ourselves (2) on Ce³⁺, Tb³⁺-codoped LaMgB₅O₁₀. Excitation into the Ce³⁺ ion is, therefore, followed by energy transfer to the Gd³⁺ sublattice. The transfer rate exceeds the Ce³⁺ radiative rate considerably in view of the absence of Ce³⁺ emission. Actually the Ce³⁺ emission peaks around 310 nm (9) and has an excellent spectral overlap with the Gd³⁺ absorption lines in that region (⁸S → ⁶P). Since the Ce³⁺ ion has a radiative decay time of about 10⁷ s⁻¹ (10), a value of 10⁹ s⁻¹ is a reasonable lower limit for the transfer rate for the distance involved (4 Å). A similar situation has been observed for GdF₃ : Ce, Tb (11).

We conclude that the Ce³⁺ ion is an excellent sensitizer for the Gd³⁺ sublattice at all temperatures. If suitable activators are built in, e.g. Tb³⁺ or Mn²⁺, they can trap the excitation energy migrating in the Gd³⁺ sublattice. In this way very efficient phosphors can be made as has been shown recently by De Hair and Van Kemenade (4).

The energy migration in the Gd³⁺ sublattice is strongly one-dimensional. To investigate this further we studied the luminescence of samples with compo-

sition (Gd,La)MgB₅O₁₀ : Tb. The La³⁺ ions which have only energy levels high above the Gd³⁺ emitting levels were thought to block effectively the one-dimensional energy migration. The Tb³⁺ ions act as traps for the migrating energy and are here used to measure the blocking of the energy migration.

(Gd, La)MgB₅O₁₀ : Tb

Figs. 3 and 4 present the results of the measurements on the system Gd_{1-x-y}La_xTb_yMgB₅O₁₀. Excitation is in the Gd³⁺ 8S → 6I transition. Plotted is the amount of Gd³⁺ emission in the total emission. Fig. 3 is for a constant Tb³⁺ concentration (y = 0.005), fig. 4 for a constant La³⁺ concentration (x = 0.7). All values plotted are at RT. At LHeT the amount of Gd³⁺ emission has increased. However, the increase of Gd³⁺ emission intensity with decreasing temperature in the lowest temperature region is very steep, so that the LHeT values are not very reliable. We were not able to perform these measurements down to 1.5 K, because the emission intensities became too weak in the specific setup used.

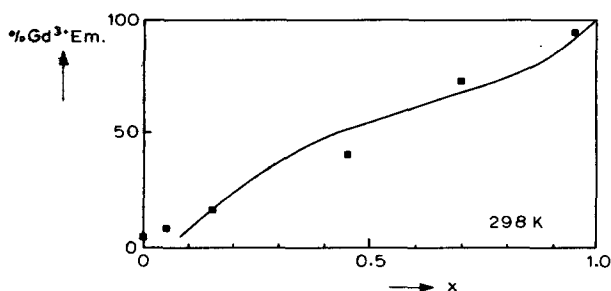


FIG. 3

The amount of Gd³⁺ emission in the total luminescence output at RT upon Gd³⁺ (8S → 6I) excitation of the system Gd_{0.995-x}La_xTb_{0.005}MgB₅O₁₀ as a function of x. Squares are experimental points. The drawn line is discussed in the text and corresponds to m = 8 and n = 60.

further here. We restrict ourselves to the room temperature results.

Fig. 3 shows that the amount of Gd³⁺ emission in the total emission depends, within the experimental accuracy, linearly on the La³⁺ concentration. At first sight this is rather surprising. If we consider the Gd³⁺ subsystem as purely onedimensional, the La³⁺ ions are expected to break the migration in the Gd³⁺ subsystem. As a consequence we expected to find a large increase of the amount of Gd³⁺ emission for a certain La³⁺ concentration. This would be similar to the observations made for the systems La_{1-x}Eu_xMgB₅O₁₀ and La_{1-x}Tb_xMgB₅O₁₀ (3). Such a model, corresponding to one-dimensional energy migration, does not seem to be applicable here.

We have searched for models which are able to explain the way in which the Gd³⁺ output depends on the La³⁺ concentration. We have not aimed at the best possible fits, but at simplicity, taking into account the transfer

rates obtained before. Let us first consider the $x = 0$ case, i.e. no La^{3+} present.

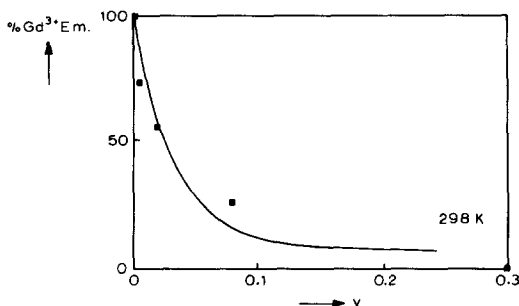


FIG. 4

The same data as in fig. 3 for the system $\text{Gd}_{0.3-y}\text{La}_{0.7}\text{Tb}_y\text{MgB}_{5-10}$ as a function of y . The curve is for $m = 8$ and $n = 20$.

chains are present, which may or may not contain Tb^{3+} ions. Such a short Gd^{3+} chain without Tb^{3+} has at first sight only one possibility to decay after excitation, viz. by radiative Gd^{3+} emission. This, however, is not correct, because $P(\text{Gd}^{3+} \rightarrow \text{Gd}^{3+} \text{ interchain}) > P(\text{Gd}^{3+}, \text{ radiative})$. For the interchain transfer rate we find $5 \cdot 10^5 \text{ s}^{-1}$ by reducing the intrachain transfer rate by a factor $(6.4/4.0)^6$, i.e. assuming electric dipole-dipole interaction. This value exceeds the radiative rate (10^3 s^{-1}).

The only model which can explain our results reasonably is the following. Consider the Gd^{3+} ions to form a system of 'chains', the length of which varies from 1 Gd^{3+} ion to arbitrary many Gd^{3+} ions. If one single Gd^{3+} ion has only La^{3+} ions on the nearest and next-nearest neighbour sites, it will yield Gd^{3+} emission. The probability for this situation is x^8 , since there are 2 nearest and 6 next-nearest neighbour sites. For 'chains' longer than one Gd^{3+} ion we neglect this possibility, since it is very small in view of the large number of neighbour sites. Because the intrachain transfer rate is high, the number of chains visited by a migrating excited Gd^{3+} state during its life time equals the square root of the ratio of the interchain transfer rate and the radiative rate, i.e. $\sqrt{5 \cdot 10^5 / 10^3} \approx 22$. This implies that the migration is by no means onedimensional.

The 22 visited chains have each two rare-earth ion sites by which they are blocked, because these sites are occupied by La^{3+} or Tb^{3+} ions. This is altogether 44 sites. If all these sites are occupied by La^{3+} ions, Gd^{3+} emission results. For the time being we assume that in all other cases Tb^{3+} emission results in view of the rather high value of $P(\text{Gd}^{3+} \rightarrow \text{Tb}^{3+})$. The probability that the 44 sites are all occupied by La^{3+} , and not by Tb^{3+} , is given by $\{x/(x+y)\}^{44}$. This model predicts the relative Gd^{3+} emission intensity

present.

For the Gd^{3+} chains the fast-diffusion model is a good approximation (see above), i.e. $P(\text{Gd}^{3+} \rightarrow \text{Gd}^{3+} \text{ intrachain}) \gg P(\text{Gd}^{3+}, \text{ radiative}), P(\text{Gd}^{3+} \rightarrow \text{Tb}^{3+})$, where $P(X)$ denotes the rate of process X . In view of the P values given above, this inequality holds. The relative amount of Gd^{3+} emission is given by $P(\text{Gd}^{3+}, \text{ radiative}) / \{P(\text{Gd}^{3+}, \text{ radiative}) + P(\text{Gd}^{3+} \rightarrow \text{Tb}^{3+}, \text{ total})\}$. The experimental value is 0.05 (fig. 3). This yields for $P(\text{Gd}^{3+} \rightarrow \text{Tb}^{3+}, \text{ total})$ about $2 \cdot 10^4 \text{ s}^{-1}$. Since the Tb^{3+} concentration $y = 0.005$, we find $P(\text{Gd}^{3+} \rightarrow \text{Tb}^{3+}) = 4 \cdot 10^6 \text{ s}^{-1}$, in excellent agreement with the value derived above.

If the La^{3+} ions break up the chains, this model can no longer be used. Between the La^{3+} ions short Gd^{3+}

to depend on the La^{3+} concentration x according to

$$x^8 + \{1-(x+y)^8\} \left(\frac{x}{x+y}\right)^{44},$$

since $(x+y)^8$ gives the fraction of isolated Gd^{3+} ions.

In order to compare this with our results, we fitted the results to the expression

$$x^m + \{1-(x+y)^m\} \left(\frac{x}{x+y}\right)^n.$$

In fig. 3 $y = 0.005$. The drawn curve in fig. 3 is for $m = 8$ and $n = 60$. This agrees reasonably well with expectation and explains the (pseudo)linear dependence of the experimental results on x .

The results of fig. 4 were also fitted. Now we find $m = 8$ and $n = 20$. The n values need a further consideration. The model assumes that, if the excitation energy reaches a Gd^{3+} chain which has a Tb^{3+} neighbour, it will be transferred to the Tb^{3+} ion. However, interchain transfer has a probability which cannot be neglected especially in view of the inaccuracy of the transfer rates which we have derived above. So the model tends to overestimate the Tb^{3+} output. This effect will be the more pronounced for the lower Tb^{3+} concentrations. The $n = 60$ value is, therefore, probably an overestimation.

In spite of all the inaccuracies involved, the model yields a satisfying understanding of the energy migration in the system $\text{Gd}_{1-x-y}\text{La}_x\text{Tb}_y\text{MgB}_5\text{O}_{10}$. Energy migration among the Gd^{3+} ions is not only intra-, but also interchain. The energy transfer $\text{Gd}^{3+} \rightarrow \text{Tb}^{3+}$ is intrachain. A spectral-overlap treatment yields for the critical distance for this transfer $\sim 5 \text{ \AA}$ using the absorption and emission spectra involved and assuming electric dipole-dipole interaction. This value agrees reasonably with the idea of intrachain $\text{Gd}^{3+} \rightarrow \text{Tb}^{3+}$ transfer.

If Ce^{3+} is used as a sensitizer of the Gd^{3+} subsystem, very efficient phosphors can be made (4). The energy migration is then of the type $\text{Ce}^{3+} \rightarrow (\text{Gd}^{3+})_n \rightarrow \text{Tb}^{3+}$, the details of which have been discussed above separately. Additional investigations have been published elsewhere (4) and lead to the same conclusions.

Finally we note that we determined the particle size of the powders, because very small particles would make the predictions of any model which implies energy migration over reasonably large distances hard to confirm. From sedimentation and X-ray absorption measurements the average particle size has found to be large enough, viz. $10 \mu\text{m}$.

Acknowledgements

Financial aid from the Academy of Finland to M.L. is acknowledged. Thanks are due to Mr. A. Pukkinen, M.Sc., Kemira Oy, for the particle size determination.

References

1. B. Saubat, M. Vlasse and C. Fouassier, *J. Solid State Chem.* 34, 271 (1980).
2. M. Saakes, M. Leskelä and G. Blasse, *Mater. Res. Bull.*, in press.
3. C. Fouassier, B. Saubat and P. Hagenmuller, *J. Luminescence* 23, 405 (1981).
4. J.Th.W. de Hair and J.T.C. van Kemenade, paper 54 at 3rd Int. Conf. Science and Technology of Light Sources, Toulouse, 1983.
5. F. Kellendonk and G. Blasse, *Phys. Stat. Sol. (b)* 108, 541 (1981).
6. M.J.J. Lammers and G. Blasse, to be published.
7. D.L. Huber, Chapter 3 in *Laser Spectroscopy of Solids* (Eds. W.M. Yen and P.M. Selzer), *Topics in Applied Physics Vol. 49*, Springer Verlag, Berlin, 1981.
8. G. Blasse, *Philips Res. Repts.* 24, 131 (1969).
9. B. Saubat, C. Fouassier, P. Hagenmuller and J.C. Bourcet, *Mat. Res. Bull.* 16, 193 (1981).
10. A. Brill, G. Blasse and J.A. de Poorter, *J. Electrochem. Soc.* 117, 346 (1970).
11. G. Blasse, *Phys. Stat. Sol. (a)* 73, 205 (1982).